UNIVERSITY OF CALIFORNIA, SAN DIEGO

Multiple Loci Contribute to Synthetic Lethality in the Zfp423 Model of Joubert Syndrome

A thesis submitted in partial satisfaction of the

requirements for the degree Master of Science

in

Biology

by

Zheng Liu

Committee in charge:

Professor Bruce Hamilton, Chair
Professor Andrew Chisholm, Co-Chair
Professor Yishi Jin

2016

The thesis of Zheng Liu is approved, and it is acceptable in quality and form for publication on microfilm and electronically:

Co-Chair

Chair

University of California, San Diego

2016

Table of Contents

List of Figures and Tables

Acknowledgement

I would first like to express my appreciation to Dr. Bruce Hamilton for giving me the opportunity to join his lab. I learned not only the skills for research, but also the attitude and passion for science during the time I have spent in the lab. Dr. Hamilton has always treated me kindly, encouraged me and offered me various support. Furthermore, I am extremely thankful for his persistence and patience throughout the edition and talk of this draft.

I would also like to thank Dr. Andrew Chisholm and Dr. Yishi Jin for being members of my committee.

I would like to thank the members of the Hamilton lab, Dorothy Conception and Kevin Ross for all of their help and support on my research questions over the years.

Lastly, I would like to thank all of my family and friends who have helped and supported me while I worked towards this graduate degree.

ABSTRACT OF THE THESIS

Multiple Loci Contribute to Synthetic Lethality in the Zfp423 Model of Joubert Syndrome

by

Zheng Liu

Master of Science in Biology

University of California, San Diego, 2016

Professor Bruce Hamilton, Chair

Professor Andrew Chisholm, Co-Chair

Zfp423 is a 30-zinc finger transcription factor with potential to integrate several canonical signaling pathways. *Nur12* mutant mice lacking *Zfp423* showed a range of clinically relevant phenotypes, which are strain dependent. The survival rate for BALB/c (BALB) is ~70%, while the survival of mutant on C57BL/6J (B6) is 0%. This

discrepancy of survival rate between BALB and B6 indicated a genetic interaction that we pursued through linkage analysis.

To identify linkage, we combined genotypes from 367 F2 intercross mutant (*nur12/nur12)* progeny of $BALB^{nur12/nur12}$ and $B6^{+/+}$ mice with genotype data from 322 previously collected F2 intercross progeny, from which we determined a need to double the sample size. We found chromosome 5 and 17 passed the significance threshold (LOD=3.4, $\alpha < 0.05$) after running a genome-wide one degree of freedom Chi-square test on the animals that are homozygous B6. We also collected survival data on 367 more recent progeny so that we could test for loci showing time-dependent contributions, for which we employed a two-part test designed for right-censored data. For the two-part analysis, chromosome 5 passed the significant threshold (LOD=3.4) and seven chromosomes passed the suggestive threshold (LOD =2.0), suggesting that multiple loci that control the quantitative trait—survival.

I.

INTRODUCTION

Zfp423 deficient mice have various defects in cerebellum, which is a component of hindbrain. It controls both coordination and balance via input from the sensory system [1]. Cerebellar disorders can be classified into developmental and degenerative disorders. Developmental disorders include congenital malformation or hypoplasia of cerebellar vermis, such as Dandy-Walker syndrome and Joubert syndrome. Degenerative disorders involve the deterioration of neurons in the cerebellum or the cerebellar atrophy, such as Huntington's disease and multiple sclerosis.

The cerebellum contains three cortical layers. The outermost layer of the cerebellar cortex is the molecular layer, which includes stellate and basket cells. The middle Purkinje layer contains only Purkinje cells. The innermost granular layer contains granule cells, unipolar brush cells and Golgi cells. The cerebellum develops from the rhombencephalon, which is the most caudal segment of the embryonic brain. There are eight rhombomeres formed during embryonic rhombencephalic segment development. The cerebellum arises from two specific rhombomeres, which are rhombomere 1 near the tail and the isthmus near the front[2]. Neurons that make up the cerebellum come from two primary regions—ventricle zone (VZ), which produces Purkinje cells and deep cerebellar neural cells and germinal zone (GZ), which is also know as Rhombic lip (RL) and produce granule cells. As development continues, the granule precursor cells that originate in the RL generate the external granule layer (EGL)[3]. This layer of cells located on the exterior of the cerebellum produces the granule neurons. Those granule cells migrate from lateral positions to form the cerebellar vermis, while cells from the VZ maintain its mediolateral position during adult cerebellum development[4].

Joubert Syndrome is one of the rare but severe brain malformations characterized by absence or immature development of an area in the medial cerebellum—cerebellar vermis—that is involved with posture and rhythmic modulation of movements and malformed brainstem—molar tooth sign[5, 6]. Most common features for the recessively inherited Joubert syndrome include congenital ataxia, abnormal breathing pattern, sleep apnea, abnormal eye and tongue movements, and even intellectual abnormality[7]. It is estimated to affect between 1 in 80,000 and 1 in 100,000 newborns [8]. However, since it has a large range of phenotypes, such as rapid breathing pattern, severity of development delay, low muscle tone and abnormal eye movements [9], some of the cases are likely under diagnosed, so the actual rate of disease might be even higher [10]. The focus of this study is a model of Joubert Syndrome 19 (JBTS19), which in human is associated with mutations in *ZNF423,* and is modeled in mice by mutations in the orthologous gene *Zfp423.*

Zfp423 is a 30 C2H2 zinc finger transcription factor with potential to integrate several canonical signaling pathways. *Zfp423* was first identified as Rat Olfactory-1 (Ebf1)-associated-zinc finger (ROAZ) by Tsai and Reed [11]. It functions different ways through the usage of three known functions, each encoded by adjacent Zinc finger domains. First, *Zfp423* can operate as a DNA-binding transcription factor through recognizing the sequence GCACCCTTGGGTGC in its DNA binding domain. Second, it can function as a Bone Morphogenic Protein (BMP) interaction transcription factor through BMP signaling domain. Lastly, it will act as an early B-cell factor (Ebf1) interaction transcription factor via a C-terminal domain that can bind Ebf1[12]. *Zfp423* binds Ebf1 as a heterodimer to repress Ebf1 to further inhibit neuronal

differentiation[13], while the Ebf1 homodimer itself will promote differentiation[14, 15]. *Zfp423* binds BMP2/BMP4-activated SMAD1 and SMAD4 as a cofactor [16], which means *Zfp423* can only bind either SMAD or Ebf1 and the two pathways are competitive[17, 18]. *Zfp423* can bind cleaved Notch intracellular domain to regulate Hes5 transcription, which is also inhibited by EBFs [19]. Retinoic acid receptors in neuroblastoma cells also bind *Zfp423*, which initiates further cell differentiation [16, 20].

Nur12 mice lacking *Zfp423* have a range of clinically relevant phenotypes, including cerebellar vermis hypoplasia, embryonic lethality [12, 21, 22] and variable loss of cerebellar hemisphere[12]. *Zfp423*-deficient animals are also defective in forebrain and midbrain development[12, 21], as well as in olfactory neurogenesis [23]. Prior work in our lab demonstrated that the presentation of phenotypes depends on genetic background and other non-genetic factors, such as environmental variation in fetal or perinatal microenvironment [12, 16]. We proposed that more of the variation was stochastic.

In addition to the effects on neurogenesis, *Zfp423* is known for its significant influence on adipogenesis—the generation of adipose tissue [24]. It is a transcriptional regulator for preadipocyte determination [24]. Both brown and white adipocyte differentiation is impaired in *Zfp423*-deficient mouse embryos and $Zfp423^{+/+}$ have more subcutaneous fat than $Zfp423^{-/-}$ mice [24].

Zfp423 mutation also results in ciliopathy-related phenotypes [25]. Our lab recently demonstrated that *Zfp423* regulates cilium function in Sonic Hedgehog (Shh) signaling [25]. Cerebellar granule cell precursors (GCPs) express *Zfp423* protein and loss of *Zfp423* inhibited their ability to respond to Shh, which altered cilium-related

functions[25]. All the studies discussed above make *Zfp423* as an important gene to study regarding different intercellular signaling pathways and disease-related models.

In prior studies, our lab observed significant survival differences depending on the strain background of *nur12* mutant mice [12]. Strikingly, the survival of mutants on BALB/c (BALB) is ~70%, while the survival of mutants on C57BL/6J (B6) is 0%. This discrepancy in survival rate indicated a genetic interaction that we pursued through linkage analysis. Our experimental setup is based on crosses between inbred lines, which are formed by repeated sibling mating to obtain individuals who are completely homozygous [26]. By crossing these strains, we obtain progeny whose genomes are shuffled versions of the parental genomes [26]. The F1 generation, obtained by crossing the two strains, has a chromosome from each parent, and all F1 individuals are genetically identical ($(BALBxB6)^{nur12/+}$). By crossing two individuals in the F1 generation, we create genetic variation in the resulting F2 population. The three possible genotypes at any one position are B6/B6, BALB/BALB and BALB/B6. A linkage map is a genetic map that shows the position of genetic markers relative to each other in terms of recombination frequency during crossover of homologous chromosomes. The greater the frequency of recombination between two markers, the further apart they are expected.

Variation in quantitative traits, such as likelihood of survival, is often due to the effects of multiple genetic loci as well as environmental factors [26]. Regions of the genome that show convincing evidence of association are considered quantitative trait loci (QTLs). We mapped QTLs by linkage in an experimental cross formed from two inbred lines—B6 and BALB—to limit complexity and allow deep sampling to detect statistically significant effects on a major phenotypic outcome: neonatal death. We

mapped QTLs with the R/qtl software package [26], an package for the R programming language commonly used in statistical computing, for the analysis of QTL experiments. QTL mapping allows for the association of phenotype and genotype in a population exhibiting genetic variation, such as the lethality rate difference between B6 and BALB mutants. In order to identify the modifier loci that contribute to the synthetic lethality, we use both one-degree of freedom Chi-square tests for categorical variables and two-part survival analysis for quantitative variables in QTL to uncover genomic regions where B6 alleles are underrepresented among surviving mutant offspring from a cross between B6 and BALB.

Evidence of linkage to a QTL is measured by a LOD score, which is the $\log_{10}$ likelihood ratio comparing the hypothesis that there is a QTL at the marker to the hypothesis that there is no QTL anywhere in the genome [26]. Large LOD scores indicate evidence for the presence of a QTL.

To map modifier loci in Zfp423 deficient mice, we developed intercross progeny from fully inbred strains. We used survival and linkage analysis to identify multiple loci that account for the difference in survival rate between BALB and B6 *Zfp423* mutants.

II.

RESULTS

Linkage identification through 1df Chi-square test across the genome

To identify linkage to survival as a binary trait, we genotyped 367 F2 intercross mutant (*nur12/nur12)* progeny of BALB$^{nur12/nur12}$ and B6$^{+/+}$ mice. We got a 98.1% genotype coverage over the whole genome so that a relatively powerful statistical analysis could be conducted with only a few missing data (Figure 1). An empirical genetic map was constructed over the mouse genome using 130 simple sequence length polymorphism (SSLP) markers from the MIT Mouse Genetic and Physical Mapping Project (Figure 2). Unlike a physical map, which specifies the physical position of markers on the chromosomes, the genetic map distance is measured by the rate of crossover events at meiosis [26]. We converted the genetic length of intervals into their recombination fractions, which relates the expected number of crossovers in an interval to the probability of an unexpected number of crossovers[26]. The map generates an average spacing of 10.6cM between markers, with the largest distance between markers at 25.1cM on chromosome 12. In regions for which the initial linkage analysis indicated some evidence for QTL (for example, middle of chromosomes 5 and tip of 17), additional markers were genotyped. We used the genotypes from our informative set of 130 SSLP markers to infer the genotypes at intervening polymorphic sites in order to identify potential QTLs. Before running any statistical analyses, suggestive and significance thresholds were declared based on Lander and Kruglyak's paper from simulation of perfect marker information [27]. Suggestive linkage means that statistical evidence expected to occur one time at random in a genome scan, while significant linkage means statistical evidence that would be expected to occur 0.05 times at random in a genome scan, which is a probability or alpha level of 5% [27].

In our study, we used the 1df Chi-square test comparing the homozygous B6 with the sum of homozygous BALB and heterozygous BALB/B6, since we are looking for locations in the genome were the homozygous B6 genotype is underrepresented. We will use significant and suggestive linkage P values (LOD) for a one-degree of freedom recessive intercross QTL mapping in mouse, which are 7.2×10^{-4} (3.4) and 2.4×10^{-3} (2.0) respectively [27].

The more recent data of 367 F2 intercross mutant progeny was visualized as a Manhattan Plot of a linkage statistic, in this case -log (p) for 1df Chi-square (Figure 3). In the middle of chromosome 5, the suggestive threshold ($P < 2.4 \times 10^{-3}$) was passed at the position of D5Mit135 and the significance threshold ($P < 7.2\times10^{-4}$) was passed at the position of rs25487227 on chromosome 5 (Table 1A). Legacy genotype data from 322 F2 intercross progeny, from which we determined to double the sample size, was combined with those more recent data to generate a more powerful test that would be more robust against error. A new Manhattan plot based on the total of 689 F2 intercross progeny was plotted (Figure 4). We found 1df Chi-square P values at positions rs254857227 on chromosome 5, D5Mit398 and D5Mit314 that passed the significance threshold ($P < 7.2\times10^{-4}$), while 1df Chi-square P values at positions D5Mit386, D5Mit233, D5Mit135 and D5Mit157 passed the suggestive threshold ($P < 2.4 \times 10^{-3}$) (Table 1B). We expect a ratio of 1 for the proportion of actual to observed homozygous B6 genotypes at each locus, assuming Mendelian inheritance, but the ratio is much lower at some loci on chromosome 5, such as rs25487227(0.672), D5Mit135 (0.706), D5Mit398 (0.747), D5Mit314 (0.746) (Table 1B). The same analysis was performed for all chromosomes and we found loci on chromosome 17 passed significance and suggestive thresholds. 1df

Chi-square P value at D17Mit113 passed the significance threshold ($P < 7.2\times10^{-4}$), while markers D17Mit164, D17Mit133 and D17Mit11 passed the suggestive threshold ($P < 2.4 \times 10^{-3}$) in the genome scan. The ratio of actual percentage of homozygous B6 and expected percentage are lower than 1 at those loci on chromosome 17, such as D17Mit113 (0.728), D17Mit164 (0.749), D17Mit133 (0.755) and D17Mit11 (0.779) (Table 2B). As a result, the magnitude of the effect also supports loci that show statistical significance, such as chromosome 5 and 17.

Comparison between Mutants and Wild Type Animals at the Same Locus.

To identify and eliminate other factors except the modifier loci that might contribute to the phenotypic difference, survival rate, between homozygous B6 mutants and homozygous BALB mutants, we extracted DNA from the wild type mice without the mutation and genotyped a few loci that showed lower 1df Chi-square P value or higher LOD value in mutants before (Table 3). None of the tested loci showed any significant association or suggestive trend in non-mutant animals. Therefore, we have evidence to support that distortion in observed frequency of B6 genotype is dependent on being *nur12/nur12.*

Two Part Analysis

To test for loci with time-dependent contributions to survival, we employed a two-part test designed for right-censored data of our more recent 367 F2 mutant progeny from $BALB^{nur12/nur12}$ and $B6^{+/+}$. Survival data was collected until 60 days and used as a quantitative trait. The two parts of the analysis are the duration of survival within 60 days and difference in genotypes among the animals that survival passes 60 days. R/qtl reports three LOD scores for the two-part analysis: lod.p, lod.mu and lod.p.mu. LOD score

represents the odds ratio of how many times the observed genotypes more likely to arise under a specified hypothesis of linkage than independent assortment [27]. Lod.p can be treated as the penetrance of the phenotype, which means given the genotype, how likely is the corresponding phenotype. Lod.mu is the severity of phenotype, which given the genotype, how big is the phenotypic difference in affected subjects. Lod.p.mu is the sum of these two effects. A genome-wide threshold on lod.p.mu is required before breaking down comparison between the two components.

In order to run the two-part analysis for right-censored survival data at 60 days, log of survival was added as a phenotype when running the test. Then log (survival) was scanned in the two-part model. For the suggestive threshold (LOD=2.0), we would expect linkage once in the whole genome scan purely by chance[27] , but we observe seven loci which pass the genome-wide suggestive threshold (Figure 5), which is unlikely to happen by chance, and supports the conclusion that multiple loci control the quantitative trait of survival. Furthermore, one of these loci on chromosome 5 passed the genome wide significance threshold (LOD=3.4) (Figure 4). If loci on chromosome 5 fully determine synthetic lethality, then these should not be homozygous B6 at the lethality loci. However, we still observed B6 genotypes for all the markers in this region, indicating chromosome 5 genotype is neither necessary nor sufficient, but it is quantitatively associated with survival. As a result, our result from the two-part analysis also suggests there are multiple loci contribute to the synthetic lethality in *Zfp423* model.

Figure 1. A. Complete genotyping of 367 F2 intercross progeny of C57BL/6J and BALB/C-*nur12*. Plot of complete genotyping information across the whole genome. At each position, black=missing genotypes, white=means complete genotype information.

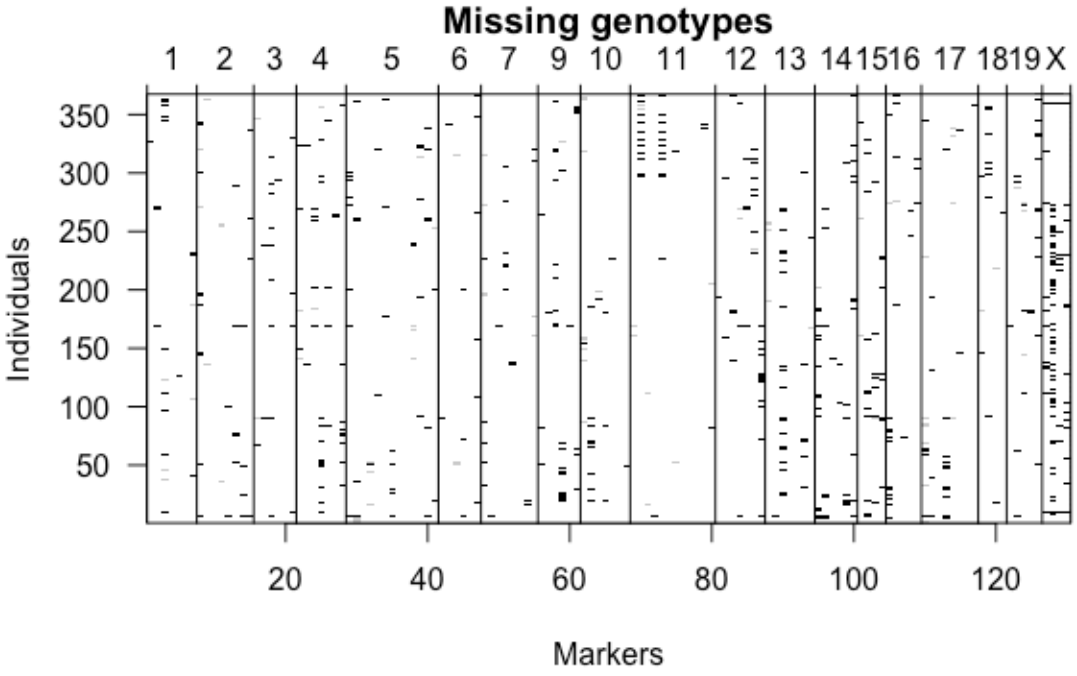
Missing genotypes
1 2 3 4 5 6 7 9 10 11 12 13 14 15 16 17 18 19 X
Individuals
350
300
250
200
150
100
50
20
40
60
80
100
120
Markers

Figure 2. Empirical genetic map of 367 F2 intercross progeny of C57BL/6J$^{+/+}$ and BALB/c$^{nur12/nur12}$. Genetic map with average markers distance of 10.6cM.

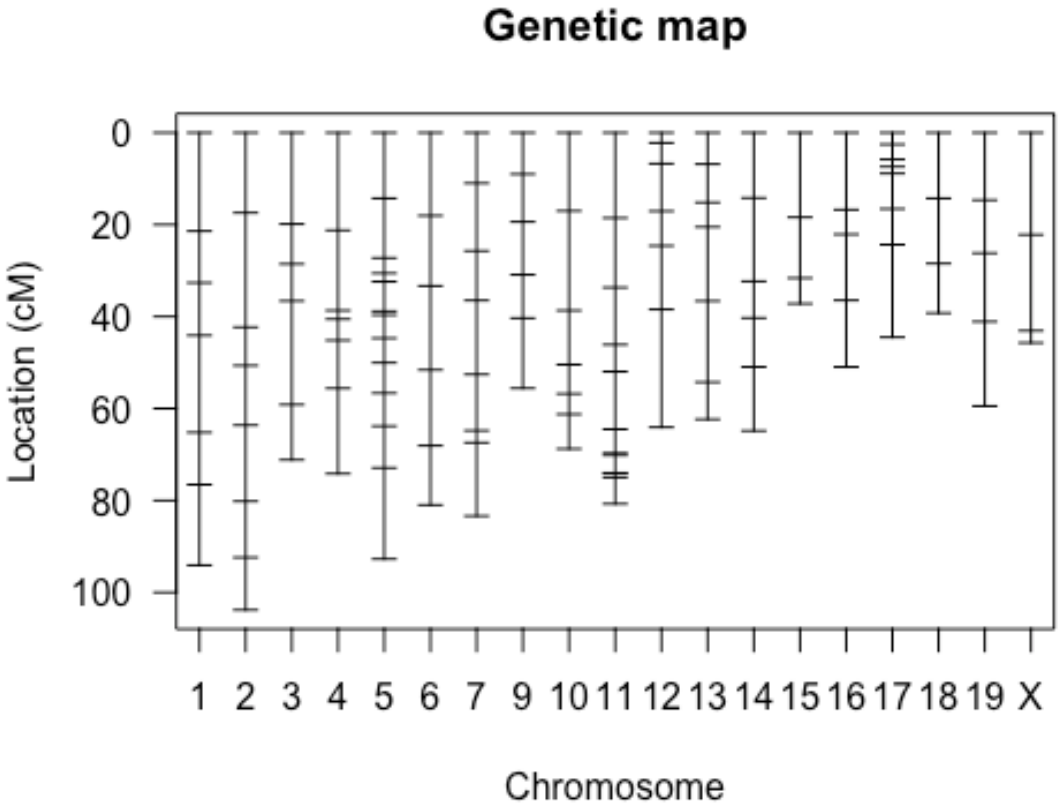
Genetic map
Location (cM)
0
20
40
60
80
100
1 2 3 4 5 6 7 9 10 11 12 13 14 15 16 17 18 19 X
Chromosome

Figure 3. Manhattan Plots of linkage data in B6$^{+/+}$×BALB$^{nur12/nur12}$ F2

A. Manhattan Plot with –log (1df) value and the position of markers on the whole genome of 367 progeny. Upper line is the significant threshold (LOD=3.4). Bottom line is the suggestive threshold (LOD=2.0).

B. Manhattan Plot with –log (1df) value and the position of markers on the whole genome of 689 progeny. Upper line is the significant threshold (LOD=3.4). Bottom line is the suggestive threshold (LOD=2.0).

A.

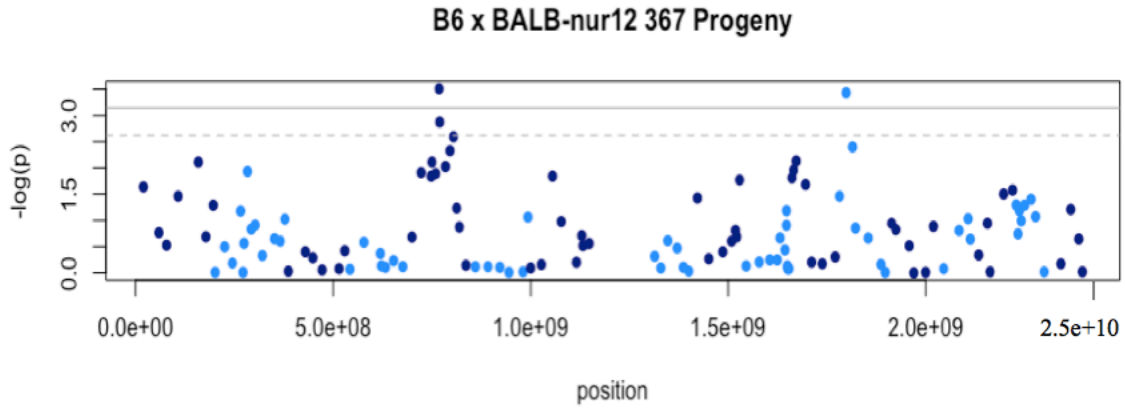
B6 x BALB-nur12 367 Progeny
-log(p)
0.0
1.5
3.0
0.0e+00
5.0e+08
1.0e+09
1.5e+09
2.0e+09
2.5e+10
position

B.

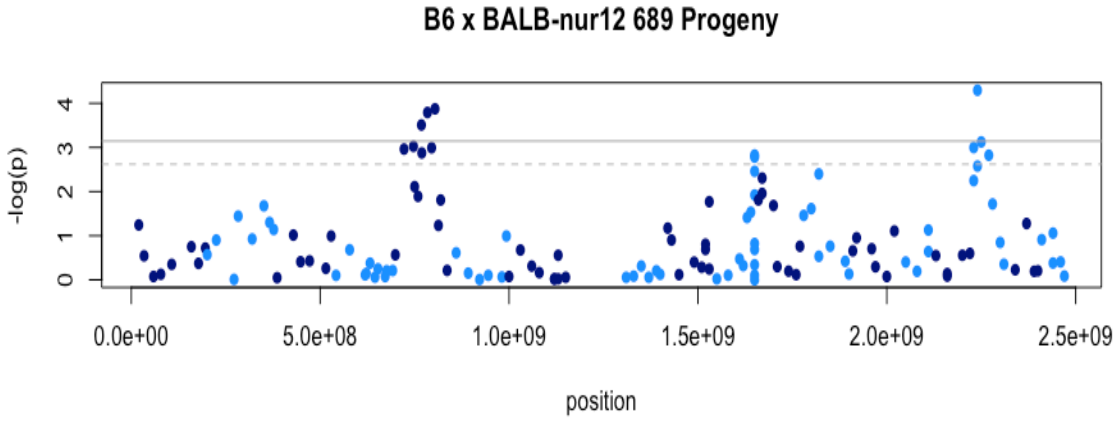
B6 x BALB-nur12 689 Progeny
-log(p)
0
1
2
3
4
0.0e+00
5.0e+08
1.0e+09
1.5e+09
2.0e+09
2.5e+09
position

Figure 4. Two part analysis for right-censored survival data at 60 days

For the 367 F2 intercross progeny of $B6^{+/+}$ and $BALB^{nur12/nur12}$, survival data until 60 days were collected and used as a quantitative trait. Using the genotype difference and the duration of survival of 60 days, two-part analysis was performed. Lod.p.mu is the sum of penetrance and severity of phenotype. Upper line is the significance threshold (LOD=3.4). Bottom line stands for the suggestive threshold (LOD=2.0).

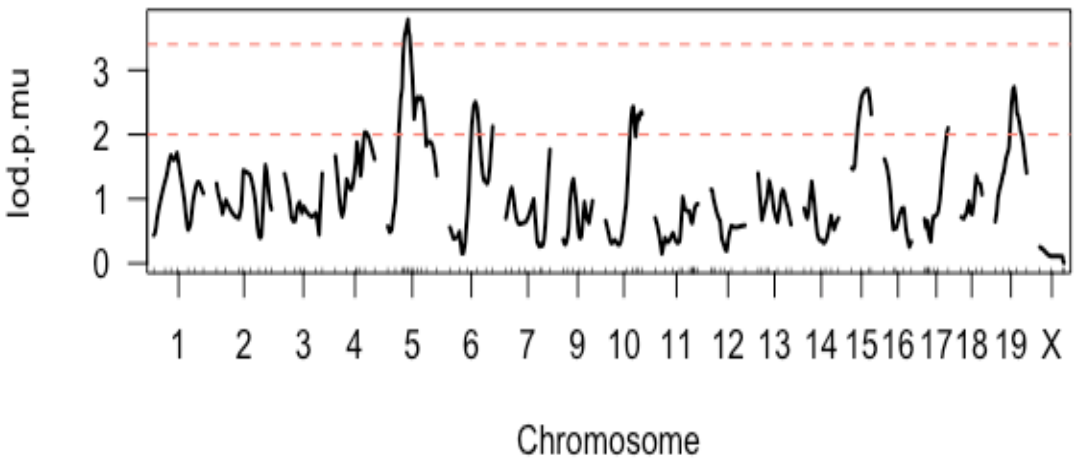
lod.p.mu
3
2
1
0
1 2 3 4 5 6 7 9 10 11 12 13 14 15 16 17 18 19 X
Chromosome

Table 1. Genotype summary on region of chromosome 5 showed significant or suggestive linkage 1df Chi-square p value.

A. One-degree of freedom chi-square p value on chromosome 5 for 367 F2 progeny

B. One-degree of freedom chi-square p value on chromosome 5 for 689 F2 progeny

A.

Markers	Position (cM)	B6	Het+BALB	(B6/Total)/0.25	1 df chi-square P value
D5Mit386	16.8	67	282	0.768	0.012
D5Mit233	31.8	71	294	0.778	0.014
rs254857227	44.0	61	302	0.676	0.00031
D5Mit135	44.8	63	290	0.706	0.0013
D5Mit398	50.1	70	296	0.756	0.0094
D5Mit157	55.8	67	294	0.742	0.0047
D5Mit314	62.8	65	294	0.724	0.0026

B.

Markers	Position (cM)	B6	Het+BALB	(B6/Total)/0.25	1 df chi-square P value
D5Mit386	17.3	126	522	0.778	0.0011
D5Mit233	33.6	130	538	0.778	0.00095
rs254857227	45.4	61	302	0.672	0.00031
D5Mit135	46.2	63	294	0.706	0.0013
D5Mit398	51.3	125	544	0.747	0.00016
D5Mit157	56.2	98	424	0.751	0.0010
D5Mit314	63.0	126	550	0.746	0.00013

Table 2. Genotype summary on region of chromosome 17 showed significant or suggestive linkage 1df Chi-square p value.

A. One-degree of freedom chi-square p value on chromosome 17 for 367 F2 progeny

B. One-degree of freedom chi-square p value on chromosome 17 for 689 F2 progeny

A.

Markers	Position (cM)	B6	Het+BALB	(B6/Total)/0.25	1 df chi-square p value
D17Mit164	1.1	71	276	0.818	0.051
D17Mit113	7.1	76	289	0.833	0.065
D17Mit213	8.7	74	275	0.848	0.10
D17Mit133	10.2	74	286	0.822	0.051
D17Mit11	18.6	74	290	0.813	0.040

B.

Markers	Position (cM)	B6	Het+BALB	(B6/Total)/0.25	1 df chi-square p value
D17Mit164	1.1	96	417	0.749	0.0010
D17Mit113	7.6	121	544	0.728	5.07E-05
D17Mit213	9.5	97	408	0.768	0.0026
D17Mit133	10.7	107	460	0.755	0.00075
D17Mit11	18.0	121	500	0.779	0.0015

Table 3. Comparison between mutants and wild type animals at the loci showed significant or suggestive linkage in F2 intercross progeny

Markers	**Mutant**		**Control (WT)**	
	1 df chisq p	-log(p)	1 df chisq p	-log(p)
D5Mit398	0.0088	2.056	0.314	0.502
D11Mit168	0.0070	2.153	0.488	0.311
D11Mit338	0.0008	3.060	0.419	0.377
D17Mit113	6.33×10^{-5}	4.198	0.347	0.459
D17Mit133	0.0026	2.582	0.394	0.404

III.

DISCUSSION

In this study, linkage was identified to multiple loci for genetic modifiers of lethality in a mouse model of Joubert Syndrome 19 (JBST19) at *Zfp423*. The survival rate was markedly different between two strain backgrounds—B6 and BALB. Genetic mapping of intercross progeny offered strong statistical support for multiple loci including those on middle of chromosome 5 and proximal end of chromosome 17 that the interaction between B6 alleles suppresses viability of *nur12* homozygotes, so fewer survivors on homozygous B6 at those loci.

We also showed evidence against modifier loci acting independently of the conditioning *nur12* mutation. However, linkage to those loci was not observed in wild type mice.

Incorporating right-censored survival data to 60 days, we are able to test if the loci show time-dependent contributions and further used two-part analysis to verify our previous findings. Chromosome 5 passed the significance threshold on both the quantitative and categorical analyses, but loci on chromosome 5 did not show complete penetrance that affect survival of *nur12* animals since there are still homozygous B6 at the lethality loci, which supports our hypothesis that there are multiple loci sufficient for survival.

We already know Zfp423 regulate PPARγ in adipose cell determination [24]. Also both brown and white adipocyte differentiation is impaired in Zfp423-deficient mouse embryos on B6 background[24]. In the future, we can look at the adipose tissue differentiation between strains and the relationship between different differentiation capacity and early mortality. There are severe brain developmental abnormalities in the *nur12* mice. From preliminary study of others in the lab, failure to survive might involve

brain stem nuclei that regulate breathing and that are sometimes affected in the cognate human disorder. As a result, we hypothesized that homeostatic oxygen function, which involve brain stem nuclei that regulate breathing, in midbrain and hindbrain is the leading suspects causing neonatal death in B6 mice. In order to solve this question, we will look at histological differences between the B6-*nur12* and BALB-*nur*12 mice brain.

Furthermore, several chromosome substitution strains (CSS) were made in our lab. We will look at CSS for chromosome 5 and chromosome 17 together and separately in B6 background in order to test whether there any loci on those chromosomes that are necessary and sufficient to cause lethality. Ten-generation fully consomic strains are available in our lab. In the future, we will use consomic and focused congenic strains to study the loci that contribute to synthetic lethality.

Genetic disorders often have several levels of noise in penetrance and severity of disease phenotypes[16]. Our results identify modifier loci that account for the phenotypic variation between different genetic backgrounds. By testing potential modifier loci in non-mutant animals, none of them showed significant association or suggestive trend, which support the deviation from the observed frequency of B6 genotypes is dependent on *nur12* mutation. Future study of those genetic modifier loci in consomic and congenic mouse strains might provide clinical insights in treating the JBST19 and other neurological developmental disorders.

IV.

MATERIALS AND METHODS

Mice. All mice in this study were kept in matching cages on hepa-filtered air in an environmentally controlled room to minimize environmental variation. All protocols were approved by UCSD Institutional Animal Care and Use Committee (IACUC) [12]. *Zfp423*$^{nur12/+}$ mice were backcrossed to BALB/C for 39 generations to get the *Zfp423*$^{nur12/nur12}$ BALB mice. Then *Zfp423*^{nur12} BALB/c were intercrossed and backcrossed to Wild Type (WT) C57BL/6J. Progeny were collected between P10 and P12. All mutants F2 and G2 generation were included in this study. For the F2 generation, mutant mice are allowed to live up 60 days and survival data was collected.

DNA Extraction and Genotyping. Mouse genomic DNA was isolated from tail biopsies. DNA was extracted by incubation in 50mM NaOH at 85℃ for three to four hours. Then DNA was neutralized with 50uL 1M Tris at pH 8.0 and diluted 1:30 in TE. Genotyping was performed using SSLP markers from MIT Mouse Genetic and Physical Mapping Project [16]. Allelic discrimination was optimal after 35 cycles of 94℃ for 15s, 55℃ for 15 and 72℃ for 30s. Expected fragment lengths are almost between 100-200 bp.

Statistical Analysis: Statistical analyses of phenotypes and genetic linkage were conducted in open source R packages (R version 3.2.4 http://www.r-project.org/). Linkage analysis was performed using the R/qtl package. Significant linkage P value is 2.4×10^{-3} and suggestive linkage P value is 7.2×10^{-4} of one-degree of freedom recessive QTL mapping in mice [27].

References

1. Buckner RL. The cerebellum and cognitive function: 25 years of insight from anatomy and neuroimaging. Neuron. 2013;80(3):807-15. Epub 2013/11/05. doi: 10.1016/j.neuron.2013.10.044. PubMed PMID: 24183029.

2. Muller F, O'Rahilly R. The human brain at stages 21-23, with particular reference to the cerebral cortical plate and to the development of the cerebellum. Anatomy and embryology. 1990;182(4):375-400. Epub 1990/01/01. PubMed PMID: 2252222.

3. Carletti B, Rossi F. Neurogenesis in the cerebellum. The Neuroscientist : a review journal bringing neurobiology, neurology and psychiatry. 2008;14(1):91-100. Epub 2007/10/04. doi: 10.1177/1073858407304629. PubMed PMID: 17911211.

4. Sgaier SK, Millet S, Villanueva MP, Berenshteyn F, Song C, Joyner AL. Morphogenetic and cellular movements that shape the mouse cerebellum; insights from genetic fate mapping. Neuron. 2005;45(1):27-40. Epub 2005/01/05. doi: 10.1016/j.neuron.2004.12.021. PubMed PMID: 15629700.

5. Yachnis AT, Rorke LB. Cerebellar and brainstem development: an overview in relation to Joubert syndrome. Journal of child neurology. 1999;14(9):570-3. Epub 1999/09/17. PubMed PMID: 10488901.

6. Brancati F, Dallapiccola B, Valente EM. Joubert Syndrome and related disorders. Orphanet journal of rare diseases. 2010;5:20. Epub 2010/07/10. doi: 10.1186/1750-1172-5-20. PubMed PMID: 20615230; PubMed Central PMCID: PMCPMC2913941.

7. Parisi MA, Dobyns WB. Human malformations of the midbrain and hindbrain: review and proposed classification scheme. Molecular genetics and metabolism. 2003;80(1-2):36-53. Epub 2003/10/22. PubMed PMID: 14567956.

8. Maria BL, Boltshauser E, Palmer SC, Tran TX. Clinical features and revised diagnostic criteria in Joubert syndrome. Journal of child neurology. 1999;14(9):583-90; discussion 90-1. Epub 1999/09/17. PubMed PMID: 10488903.

9. Fennell EB, Gitten JC, Dede DE, Maria BL. Cognition, behavior, and development in Joubert syndrome. Journal of child neurology. 1999;14(9):592-6. Epub 1999/09/17. PubMed PMID: 10488904.

10. Aslan H, Ulker V, Gulcan EM, Numanoglu C, Gul A, Agar M, et al. Prenatal diagnosis of Joubert syndrome: a case report. Prenatal diagnosis. 2002;22(1):13-6. Epub 2002/01/26. PubMed PMID: 11810643.

11. Tsai RY, Reed RR. Identification of DNA recognition sequences and protein interaction domains of the multiple-Zn-finger protein Roaz. Molecular and cellular biology. 1998;18(11):6447-56. Epub 1998/10/17. PubMed PMID: 9774661; PubMed Central PMCID: PMCPMC109231.

12. Alcaraz WA, Gold DA, Raponi E, Gent PM, Concepcion D, Hamilton BA. Zfp423 controls proliferation and differentiation of neural precursors in cerebellar vermis formation. Proc Natl Acad Sci U S A. 2006;103(51):19424-9. doi: 10.1073/pnas.0609184103. PubMed PMID: 17151198; PubMed Central PMCID: PMCPMC1748242.

13. Tsai RY, Reed RR. Cloning and functional characterization of Roaz, a zinc finger protein that interacts with O/E-1 to regulate gene expression: implications for olfactory neuronal development. The Journal of neuroscience : the official journal of the Society for Neuroscience. 1997;17(11):4159-69. Epub 1997/06/01. PubMed PMID: 9151733.

14. Wang SS, Lewcock JW, Feinstein P, Mombaerts P, Reed RR. Genetic disruptions of O/E2 and O/E3 genes reveal involvement in olfactory receptor neuron projection. Development (Cambridge, England). 2004;131(6):1377-88. Epub 2004/03/03. doi: 10.1242/dev.01009. PubMed PMID: 14993187.

15. Garcia-Dominguez M, Poquet C, Garel S, Charnay P. Ebf gene function is required for coupling neuronal differentiation and cell cycle exit. Development (Cambridge, England). 2003;130(24):6013-25. Epub 2003/10/24. doi: 10.1242/dev.00840. PubMed PMID: 14573522.

16. Alcaraz WA, Chen E, Valdes P, Kim E, Lo YH, Vo J, et al. Modifier genes and non-genetic factors reshape anatomical deficits in Zfp423-deficient mice. Hum Mol Genet. 2011;20(19):3822-30. doi: 10.1093/hmg/ddr300. PubMed PMID: 21729880; PubMed Central PMCID: PMCPMC3168291.

17. Hata A, Seoane J, Lagna G, Montalvo E, Hemmati-Brivanlou A, Massague J. OAZ uses distinct DNA- and protein-binding zinc fingers in separate BMP-Smad and Olf signaling pathways. Cell. 2000;100(2):229-40. Epub 2000/02/05. PubMed PMID: 10660046.

18. Ku M, Howard S, Ni W, Lagna G, Hata A. OAZ regulates bone morphogenetic protein signaling through Smad6 activation. The Journal of biological chemistry. 2006;281(8):5277-87. Epub 2005/12/24. doi: 10.1074/jbc.M510004200. PubMed PMID: 16373339.

19. Masserdotti G, Badaloni A, Green YS, Croci L, Barili V, Bergamini G, et al. ZFP423 coordinates Notch and bone morphogenetic protein signaling, selectively up-regulating Hes5 gene expression. The Journal of biological chemistry.

2010;285(40):30814-24. Epub 2010/06/16. doi: 10.1074/jbc.M110.142869. PubMed PMID: 20547764; PubMed Central PMCID: PMCPMC2945575.
20. Huang S, Laoukili J, Epping MT, Koster J, Holzel M, Westerman BA, et al. ZNF423 is critically required for retinoic acid-induced differentiation and is a marker of neuroblastoma outcome. Cancer cell. 2009;15(4):328-40. Epub 2009/04/07. doi: 10.1016/j.ccr.2009.02.023. PubMed PMID: 19345331; PubMed Central PMCID: PMCPMC2693316.

21. Cheng LE, Zhang J, Reed RR. The transcription factor Zfp423/OAZ is required for cerebellar development and CNS midline patterning. Developmental biology. 2007;307(1):43-52. Epub 2007/05/26. doi: 10.1016/j.ydbio.2007.04.005. PubMed PMID: 17524391; PubMed Central PMCID: PMCPMC2866529.

22. Warming S, Rachel RA, Jenkins NA, Copeland NG. Zfp423 is required for normal cerebellar development. Molecular and cellular biology. 2006;26(18):6913-22. Epub 2006/09/01. doi: 10.1128/mcb.02255-05. PubMed PMID: 16943432; PubMed Central PMCID: PMCPMC1592861.

23. Cheng LE, Reed RR. Zfp423/OAZ participates in a developmental switch during olfactory neurogenesis. Neuron. 2007;54(4):547-57. Epub 2007/05/25. doi: 10.1016/j.neuron.2007.04.029. PubMed PMID: 17521568; PubMed Central PMCID: PMCPMC2866517.

24. Gupta RK, Arany Z, Seale P, Mepani RJ, Ye L, Conroe HM, et al. Transcriptional control of preadipocyte determination by Zfp423. Nature. 2010;464(7288):619-23. Epub 2010/03/05. doi: 10.1038/nature08816. PubMed PMID: 20200519; PubMed Central PMCID: PMCPMC2845731.

25. Hong CJ, Hamilton BA. Zfp423 Regulates Sonic Hedgehog Signaling via Primary Cilium Function. PLoS genetics. 2016;12(10):e1006357. Epub 2016/10/12. doi: 10.1371/journal.pgen.1006357. PubMed PMID: 27727273; PubMed Central PMCID: PMCPMC5065120.

26. Broman KW, Sen S. A guide to QTL mapping with R/qtl. Dordrecht ; New York: Springer,; 2009. Available from: SpringerLink. Restricted to UC campuses http://dx.doi.org/10.1007/978-0-387-92125-9.

27. Lander E, Kruglyak L. Genetic dissection of complex traits: guidelines for interpreting and reporting linkage results. Nature genetics. 1995;11(3):241-7. Epub 1995/11/01. doi: 10.1038/ng1195-241. PubMed PMID: 7581446.